

Identification of novel inhibitory metabolites and impact verification on growth and protein synthesis in mammalian cells

Bingyu Kuang^{a,1}, Venkata Gayatri Dhara^{b,1}, Duc Hoang^a, Jack Jenkins^b, Pranay Ladiwala^b, Yanglan Tan^c, Scott A. Shaffer^c, Shaun C. Galbraith^a, Michael J. Betenbaugh^{b,2}, Seongkyu Yoon^{a,*,2}

^a Department of Chemical Engineering, University of Massachusetts Lowell, Lowell, MA, 01854, USA

^b Department of Chemical and Biomolecular Engineering, Johns Hopkins University, Baltimore, MD, 21218, USA

^c Department of Biochemistry and Molecular Pharmacology, University of Massachusetts Medical School, Shrewsbury, MA, 01545, USA

ARTICLE INFO

Keywords:

Inhibitory metabolites
Metabolomics
Mammalian cell culture
Amino acid metabolism
Glycolysis
Process development

ABSTRACT

Mammalian cells consume large amount of nutrients during growth and production. However, endogenous metabolic inefficiencies often prevent cells to fully utilize nutrients to support growth and protein production. Instead, significant fraction of fed nutrients is diverted into extracellular accumulation of waste by-products and metabolites, further inhibiting proliferation and protein synthesis. In this study, an LC-MS/MS based metabolomics pipeline was used to screen Chinese hamster ovary (CHO) extracellular metabolites. Six out of eight identified inhibitory metabolites, caused by the inefficient cell metabolism, were not previously studied in CHO cells: aconitic acid, 2-hydroxyisocaproic acid, methylsuccinic acid, cytidine monophosphate, trigonelline, and n-acetyl putrescine. When supplemented back into a fed-batch culture, significant reduction in cellular growth was observed in the presence of each metabolite and all the identified metabolites were shown to impact the glycosylation of a model secreted antibody, with seven of these also reducing CHO cellular productivity (titer) and all eight inhibiting the formation of mono-galactosylated biantennary (G1F) and biantennary galactosylated (G2F) N-glycans. These inhibitory metabolites further impact the metabolism of cells, leading to a significant reduction in CHO cellular growth and specific productivity in fed-batch culture (maximum reductions of 27.2% and 40.6% respectively). In-depth pathway analysis revealed that these metabolites are produced when cells utilize major energy sources such as glucose and select amino acids (tryptophan, arginine, isoleucine, and leucine) for growth, maintenance, and protein production. Furthermore, these novel inhibitory metabolites were observed to accumulate in multiple CHO cell lines (CHO-K1 and CHO-GS) as well as HEK293 cell line. This study provides a robust and holistic methodology to incorporate global metabolomic analysis into cell culture studies for elucidation and structural verification of novel metabolites that participate in key metabolic pathways to growth, production, and post-translational modification in biopharmaceutical production.

1. Introduction

Biotherapeutics have emerged as one of the most effective treatment options for many diseases including cancers and autoimmune disorders. For more than three decades, mammalian production hosts have been used to produce these biotherapeutic molecules (Dhara et al., 2018). Of these hosts, Chinese hamster ovary (CHO) cells are used extensively at production scale to produce a majority of therapeutic proteins, such as

monoclonal antibodies. The market value of CHO-expressed therapeutic proteins is expected to reach \$217 billion by 2023 (Grilo and Mantalaris, 2019). This coupled with their biocompatibility through human-like post-translational modifications by the CHO cellular production machinery, make them the preferred hosts in the biopharmaceutical industry. Maximizing the protein producing capacity of the cells has been pursued in several ways such as supplementing cell growth medium with growth and productivity enhancers (Takagi et al., 2017), changing the operating mode of cell culture to fed-batch and perfusion (Hiller et al.,

* Corresponding author.

E-mail address: Seongkyu.Yoon@uml.edu (S. Yoon).

¹ These authors contributed equally.

² These authors jointly supervised this work.

<https://doi.org/10.1016/j.mec.2021.e00182>

Received 15 June 2021; Received in revised form 24 August 2021; Accepted 26 August 2021

Available online 6 September 2021

2214-0301/© 2021 Published by Elsevier B.V. on behalf of International Metabolic Engineering Society. This is an open access article under the CC BY-NC-ND

license (<http://creativecommons.org/licenses/by-nc-nd/4.0/>).

Abbreviation

ACA – aconitic acid
 Aco2 – aconitase
 BCAA – branched-chain amino acid
 CHO – Chinese hamster ovary
 CMP – cytidine monophosphate
 G1F – mono-galactosylated
 G2F – biantennary galactosylated
 GEM – genome scale model
 GMP – guanosine monophosphate
 HCD – high cell density
 HEK293 – human embryonic kidney 293
 HICA – 2-hydroxyisocaproic acid

ICA – indole-3-carboxylic acid
 IVCD – integral viable cell density
 LC-MS – liquid chromatography - tandem mass spectrometry
 MS – mass spectrometry
 MSA – methylsuccinic acid
 NAP – n-acetylputrescine
 P5C – 1-pyrroline-5-carboxylate
 PYCR – pyrroline-5-carboxylate reductase
 RSD – relative standard deviation
 RT – retention time;
 TCA cycle – tricarboxylic acid cycle
 TRI – trigonelline;
 VCD – viable cell density

2017), and optimizing the cellular environment (e.g. temperature, dissolved oxygen, pCO₂, pH, etc.) to increase its longevity and productivity (Mohan et al., 2008).

Such process improvements have enabled the industry to reach very high viable cell densities in the order of 10⁷ cells·mL⁻¹, with production yields of several grams per liter (Kunert and Reinhart, 2016). Despite these improvements, limitations still exist in the productive capacity of the cells. One possible avenue to increase cellular productivity is addressing inefficient metabolism of available substrates (such as glucose and glutamine) in the cells, leading to the production and accumulation of waste metabolites over the duration of the cell culture (Pereira et al., 2018). CHO cells exhibit inefficient and poorly regulated metabolism if they consume more nutrients than required to support proliferation and production and thereby generate waste metabolites. Such inefficient metabolism can lead to the accumulation of potentially toxic metabolites which can inhibit overall cellular performance, especially at later stages of the culture process (Pereira et al., 2018). The impacts of undesired end-products such as lactate or ammonia have been widely reported (Lao and Toth, 1997; Chen and Harcum, 2005; Sun and Zhang, 2001; Freund and Croughan, 2018; Buchsteiner et al., 2018). These by-products can become major rate-limiting factors, hindering further constructive utilization of the substrates or a decline in cellular performance with respect to cell proliferation and/or antibody production. To better regulate cell metabolism throughout the process and enhance cellular productivity, it is crucial to identify all inhibitory waste metabolites, study their corresponding biochemical precursors and evaluate their pathways of generation.

Liquid chromatography with tandem mass spectrometry (LC-MS/MS) is a powerful tool for analyzing potentially thousands of metabolites from a single sample. Owing to this, LC-MS/MS has been used in various metabolomic studies to identify markers in CHO cells which enhance growth and/or productivity. Recent study has shown LC-MS/MS can be used for quantitative assessments of medium additives and nutrients (Hoang et al., 2021). Additionally, LC-MS/MS has also been demonstrated to be capable of providing insights into cellular metabolism by profiling the extracellular metabolites generated during growth of CHO cells (Mohmad-Saberi et al., 2013). LC-MS/MS-based metabolomics can also probe the metabolic states of CHO cells by identifying growth limiting factors during different stages of culturing, including but not limited to oxidative stress and lipid metabolism (Chong et al., 2012). Other studies applied quantitative metabolomics to evaluate perfusion cell culture, which established a relationship between the multiple steady states in the process (Karst et al., 2017). Identification of metabolic by-products in CHO cell cultures that accumulate to toxic levels in CHO cell fed-batch processes and impact the culture performance has also been enabled through LC-MS/MS (Chong et al., 2011). Additionally, it has been shown that the extracellular environment is critical for cell proliferation and product titer quality in mammalian bioprocesses

(Arden and Betenbaugh, 2004; Polanco et al., 2020). A recent study has demonstrated that accumulation of by-products such as isovalerate, indolelactate, indole-3-carboxylate, and others in high-density CHO cell fed-batch process was emerged from degradation of various essential amino acids such as leucine, tyrosine, and tryptophan (Mulukutla et al., 2017). Buildup of such waste inhibitory products inhibits cell culture performance and hinders productivity and thus, preventing or reducing the accumulation of these by-products will improve process performance. Therefore, it is of paramount importance to identify the inhibitory metabolites accumulated in mammalian bioprocess, and therefore unfolding the correlation between downstream metabolites to upstream feeding source.

In this study, LC-MS/MS based untargeted metabolomics platform is used to investigate the extracellular environment of a fed-batch CHO-K1 cell culture process to identify metabolites accumulating over the culture duration. Seventeen novel accumulating metabolites were tested for cell culture toxicity. A targeted metabolomic analysis was then used to confirm these results and eight were observed to quantifiably accumulate and negatively impact growth and antibody productivity. Sensitivity and pathway analysis on CHO-GS, CHO-K1, and HEK293 cell lines confirmed these inhibitory metabolites are not exclusive to CHO-K1 but can also be found across different mammalian host systems. The methodology developed here (see Fig. 1), as well as the metabolites identified which can be used to overcome growth and production bottlenecks in CHO and other mammalian production hosts can provide the foundation for development of robust future biomanufacturing platforms.

2. Materials and methods

2.1. Cells, media, and supplements

A CHO-K1 cell line expressing IgG (VRC01) antibody obtained from NIH (National Institute of Health) was used for this study with two proprietary media. For inoculation, basal medium (medium A) obtained from Sigma Aldrich (St. Louis, MO) and glutamine at 8 mM obtained from Corning (Corning, NY) were supplemented to cell culture on Day 0. For fed-batch process, enriched nutrient feed medium (medium B) obtained from Lonza (Portsmouth, NH) was used as feed medium and fed to cells after Day 0 until cellular viability dropped below 80%. The initial feeding day is dependent on the development of feeding strategy and is clearly addressed throughout the discussion. Cells were cultivated in sterile 125 mL shake flask obtained from Fisher Scientific (Waltham, MA) with a working volume of 30 mL in a humidified, shaking incubator (Model AJ125) obtained from ATR Biotech (Laurel, MD) operated at 125 RPM, 36.5 °C, and 5.2% carbon dioxide. Cells were inoculated at low viable cell densities (VCD) (approximately 0.5 × 10⁶ cells·mL⁻¹) in basal medium and harvested when cell viability decreased below 80%. Sub-culturing was done every two to three days when the cells reached

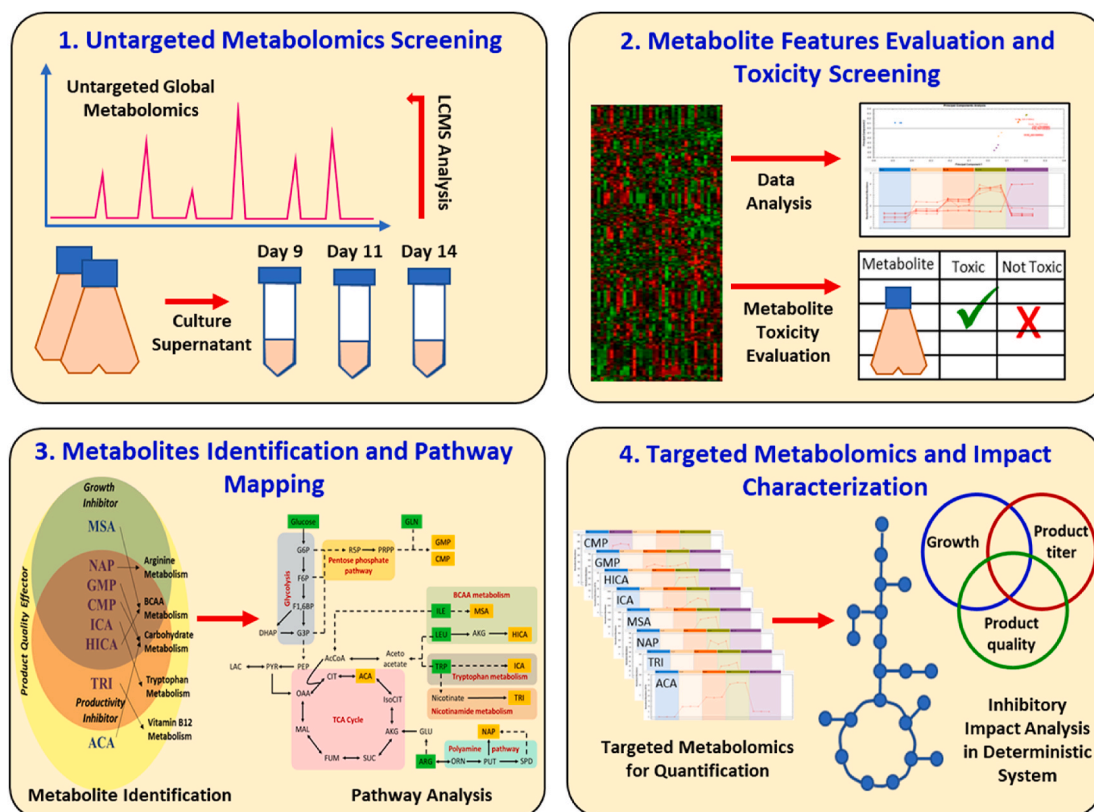


Fig. 1. Proposed metabolomics platform for identification of inhibitory metabolites in CHO bioprocess. Cell culture samples are collected, after which culture supernatant are screened through LC-MS for untargeted identification of potential metabolite features. Metabolites impact screening study is conducted on candidate metabolite features to verify their inhibitory impact on CHO cultures. Metabolites that show no inhibitory effect on CHO cultures, elucidated through spike-in study, are further considered in downstream metabolomics pipeline. Pathway analysis study is conducted on metabolites identified to be growth or productivity inhibitors, after which metabolites are mapped to their pathway of generation for identification of their metabolic precursors. Finally, inhibitory metabolites impact characterization is conducted on CHO fed-batch process to characterize inhibitory impact of metabolites on growth, titer productivity and titer quality due to exposure of cells to inhibitors for a prolonged period.

VCD greater than 3×10^6 cells·mL⁻¹. Cell viability was maintained above 90% throughout the inoculation phase. Stock solution of each candidate metabolite was prepared by dissolving pure metabolite standards obtained from Sigma Aldrich (St. Louis, MO) into ultrapure water from a MilliQ water purifier obtained from Millipore Sigma (Burlington, MA), and were supplemented in the basal media on Day 0 for both batch and fed-batch processes. For process validation, a CHO-S cell line cultured in medium A, and HEK293 cell line (CRL-1573.3) obtained from American Type Culture Collection (Manassas, VA) cultured in Irvine BalanCD medium obtained from Irvine Scientific (Santa Ana, CA).

2.2. Assessment of growth and productivity

VCD and viability were measured daily with a cell counter device (CeDex HiRes) obtained from Roche (Branchburg, NJ). Glucose, lactate, and ammonia concentration data from each culture condition were measured using an analyzer (Bioprofile FLEX) obtained from Nova Biomedical (Waltham, MA). Titer analysis was performed using a high-pressure liquid chromatography system (Agilent 1100 series) obtained from Agilent Technologies (Santa Clara, CA) with a protein A column (Poros A, 2 μ m, 2.1 \times 30 mm) obtained from Thermo Scientific (Waltham, MA). Cell culture supernatant samples were collected at different days for metabolomic analysis and titer was analyzed on the harvest day. The integral viable cell density (IVCD) at day n was defined as the summation of VCD for each day during CHO cell culture up until day n . To compare and evaluate the performance of each culture condition, the productivity at day n was calculated – defined as the overall measured titer (mg·L⁻¹) normalized against IVCD at day n .

2.3. Glycan analysis

Human serum IgG reference standard, 2-aminobenzamide (2AB), 2-picolone borane complex (2 PB), ammonium formate and acetonitrile (HPLC-grade) were obtained from Sigma Aldrich (St. Louis, MO). Magnetic beads coated with protein A and protein G were purchased from Thermo Fisher Scientific (Waltham, MA). A peptide:N-glycosidase F (PNGase F) enzyme kit containing 10 \times denaturing buffer, NP-40 non-ion surfactant detergent and 10 \times reaction buffer was purchased from New England Biolabs (Ipswich, MA) and stored as instructed by the manufacturer. Diol solid phase extraction cartridges HyperSep™ Diol SPE were purchased from Thermo Fisher Scientific (Waltham, MA). Glycocalclean™ S cartridges were from Prozyme (Hayward, CA). An inline filter (0.2 μ m) was purchased from Restek Corporation (Bellefonte, PA) and a BEH amide column (1.7 μ m, 2.1 mm \times 50 mm) was purchased from Waters Corporation (Milford, MA). For summary of a detail protocol, interested reader can refer to **Supplement S2**.

2.4. Protein purification

The method for glycan analysis was followed closely to a previously established protocol (Sha et al., 2020). Simply put, cell culture samples were collected to contain approximately 0.1–0.5 g L⁻¹ titer (about 100–500 μ L supernatant) to a 1.5 mL microcentrifuge tube, after which samples were spun down for 5 min at 1000 rpm. The supernatant which contained IgG was collected to a microcentrifuge tube, into which an aliquot of 10 μ L magnetic bead slurry was added. The beads were washed twice, each time with 250 μ L buffer. A magnetic stand was

incorporated into each wash to separate the beads from the buffer, after which the washing eluent was discarded. A volume of culture supernatant was calculated to contain approximately 20–50 µg mAb is then added to 1.5 mL microcentrifuge tube, after which the tube was vortexed gently and incubated on a shaker for 15 min. The tube was placed on the magnetic stand to separate the beads-IgG complex from the supernatant, after which the supernatant was removed. The beads were washed by two consecutive washes, with the first wash using 250 µL of binding buffer following by a second wash of 250 µL water. The beads were further suspended into 25 µL of elution buffer and incubated for 10 min. The tube was then placed on the magnetic stand and the supernatant (free of magnetic beads) is transferred to a new microcentrifuge tube which was pre-loaded with 8 µL neutralization buffer.

2.5. Enzymatic digestion of N-linked glycan from glycoprotein

Purified standard/mAbs solution is denatured by adding 4 µL of 10× denaturing buffer purchased from New England Biolabs (Ipswich, MA) and 6 µL of water. The mixture was then heated at 100 °C for 10 min. After cooling for 15 min, the mixture was added with 5 µL of 10× PNGase F reaction buffer and 5 µL of NP-40 in water. Water was added to the sample to reach a final 50 µL reaction volume. The PNGase F enzyme is added at 1 µL (500,000 units·mL⁻¹), after which the digestion was carried out at 37 °C for 20 min.

2.6. Glycan labeling and cleanup procedure

The labeling solution was prepared to a final composition containing 0.35 M of 2AB, 1 M of 2 PB, 30% vol/vol (v/v) acetic acid in 70% DMSO. Labeling solution was added at 50 µL–50 µL of the digested protein solution, after which the mixture was covered with aluminum foil and incubated at 65 °C for 1 h.

For 2AB cleanup, the methodology presented in this paper utilized Diol SPE cartridge as an economical substitute to HILIC cartridge as previous study has reported a similar and comparable final results (Sha et al., 2020). To use Diol SPE for sample cleanup, the cartridges were attached to a vacuum manifold equipped with a vacuum pump. The cartridges were first washed with 1 mL of water, followed by four consecutive washes of 1 mL ACN each wash. Labeled glycans were diluted in ACN at a ratio of 10/90% v/v. Sample were then loaded and pumped through the cartridge, after which two washes of 500 µL ACN each wash was added to remove unbound compounds including excess 2-AB. Finally, two consecutive aliquots of 100 µL water were added to elute the labeled glycans into fresh 1.5 mL microcentrifuge tube. The total volume of the eluent is 200 µL.

2.7. LC-MS/MS method for metabolites profiling

Metabolite standards were obtained from Sigma Aldrich (St. Louis, MO) and used for identification of inhibitor metabolites. Labeled amino acid standards set A (NSK-A) obtained from Cambridge Isotope Laboratories (Tewksbury, MA) was dissolved in water to prepare internal standards (IS) solution. IS solution of glycine (¹³C, ¹⁵N) was prepared at 5 M. The remaining labeled amino acid IS was prepared at 1 M. Samples were prepared by mixing 20 µL of sample with 5 µL IS and 100 µL Acetonitrile. Samples were vortexed for 30 s and centrifuged for 10 min at 16,000 g. The supernatant was then extracted for LC-MS/MS analysis.

For MS analysis, 3 µL of sample was analyzed through orbitrap LC-MS system (Thermo Scientific Accela) consisting of a LC column and a linear trap quadrupole mass spectrometer obtained from Thermo Scientific (Waltham, MA). Chromatographic separation was performed on a PEEK coated column (SeQuant ZIC-CHILIC, 3 µm, 100 × 2.1 mm) with a guard kit (SeQuant ZIC-CHILIC, 5 µm, 20 × 2.1 mm), both obtained from Millipore Sigma (Burlington, MA). For detail operating conditions regarding quantification method, interested reader can refer to **Supplements S2**.

2.8. Global metabolomics study

Hydrophilic metabolites (e.g., ACA derivatives, organic acids, sugars, and pyrimidines) were studied in the metabolome of HCD CHO fed-batch process using high resolution Orbitrap LC-MS system obtained from Thermo Scientific (Waltham, MA). Metabolomic data obtained through LC-MS were mapped to the human metabolome database (HMDB) to reveal additional metabolomic features. Overall, more than 30,000 hits were revealed using the Scaffold Elements software obtained from Proteome Software (Portland, OR). As an effort to acquire high-confidence metabolites identification in subsequent targeted metabolomic study and biological toxicity test, an MS2 scoring system was incorporated into the analysis, as used in previous studies (Huang et al., 2020). The MS2 score of each metabolite is determined by comparing MS2 precursor record from the database to every MS2 scan through a dot product between the databased recorded MS2 fragment scan and experimental analyte fragment MS2 scan.

For the untargeted global metabolomic study, since both types of mediums (medium A and medium B) were used simultaneously throughout different processes presented in this study, the MS signal intensity of both mediums are therefore normalized by constructing a blank consisted of medium A and medium B added to a final of volume with composition of medium A/medium B = 1/1.4 %v/v. Thus, the downstream ion intensity of each metabolite (*I_i*) is defined to be the detected ion intensity obtained from orbitrap MS subtracting the ion intensity of the blank. The standard deviation (*σ*) and average intensity value (*Ī*) of each metabolite *i* are calculated from triplicate measurements, from which the relative standard deviation (RSD) for each metabolite can be calculated (Eq (1)).

$$RSD = \frac{\sigma}{\bar{I}} \quad (1)$$

2.9. Impact determination and metabolite characterization

CHO-K1 and CHO-S cultures were cultivated in their respective media (CHO-K1 in medium A and CHO-GS in modified medium A). Both media were supplemented with 6–8 mM of glutamine (Corning INC, Corning, NY). Cells were cultured in 125 mL Erlenmeyer flask obtained from Fisher Scientific (Waltham, MA) with a working volume of 30 mL. Sub-culturing of cells was performed every two to three days when cells reached VCD of more than 3 × 10⁶ cells·mL⁻¹. All the metabolites screened for the spike-in studies and confirmation batch runs were obtained in pure forms from Millipore Sigma (Burlington, MA) and are listed in **Table S 2**. To examine the impact of metabolites for the screening studies, the metabolites were spiked into the CHO cell cultures at two different concentrations (1 mM and 5 mM). Whereas, during metabolite characterization studies, an additional level was tested taken from the measured accumulation levels of the inhibitory metabolite from targeted metabolomics performed on CHO-K1 fed-batch cultures. Stock solutions of metabolites (except for trans-cinnamic acid and hydroxyphenyllactic acid due to their low solubility) were dissolved with water or DMSO depending on compound solubility. The solutions were added to the culture on Day 0. The pH of the medium was adjusted to minimize the effect of pH changes resulting from the metabolite additions. The inhibitor-spiked media were evaluated for osmolality, verifying a minimal change of less than 10% in osmolality (less than 4% on average), which remains well within the acceptable range of cell culture media osmolality variation. Cells were inoculated at a seeding cell density of 0.5 × 10⁶ cells·mL⁻¹. Samples were collected for cell count and metabolite measurement every 24 h. Cell count was performed using a hemocytometer until the viability dropped below 70%. Spent medium analysis for glucose and lactate measurements was performed using a biochemistry analyzer obtained from YSI (Yellow Springs, OH). All the conditions were tested with biological duplicates and the flasks were maintained at 37 °C in a humidified shaker incubator.

obtained from Infors HT (Weymouth, MA) at 5% CO₂ levels.

3. Results and discussion

3.1. High cell density process development

A high cell density (HCD) fed-batch process was conducted with nine different feeding conditions on a CHO-K1 cell line using medium A, as illustrated in Table 1. When studied the effect of different feeding volumes on cell culture performance, the study found that medium feeding condition (condition 5, feeding volume 3 mL) resulted in the highest IVCD (see Fig. 2 B), which was 30.8% higher than the high feeding condition (condition 3, feeding volume 4.5 mL) and 25.9% higher than the low feeding condition (condition 7, feeding volume 1.5 mL). High feeding volume was found to be directly correlated to higher glucose consumption and lactate accumulation rate when compared against the medium and low feeding condition (see Fig. 2 C and D). However, high feeding volume did not translate to a better growth profile, as the medium feeding condition (feeding volume 3 mL) showed highest VCD and growth rate (Fig. 2 A). Similarly, when studied the effect of different initial feeding day, the study found that feeding on Day 3 (condition 5) resulted in the highest attainable cumulative IVCD (see Fig. 2 F), which was 11.8% higher than the early feeding condition (condition 2, Day 2) and 10.9% higher than the late feeding condition (condition 8, Day 4) with all three conditions maintaining the same 3 mL feeding amount. Feeding too early (condition 2, feeding Day 2) resulted in cells reaching production phase at lower peak VCD. On the other hand, feeding too late (condition 8, feeding Day 4) resulted in cells rapidly reaching highest peak VCD (Day 8) but rapidly approaching death phase and consequently translated to the shortest culture duration (12 days culture duration, Fig. 2 E). A similar metabolism profile was also observed when the effect of different initial feeding days on cellular performance was studied, as the earliest feeding day (condition 2, feeding Day 2) with the most abundant nutrients available in the spent medium allowed cells to up-regulate their glycolysis pathway (higher glucose uptake) and higher lactate production when compared against the mid and late feeding conditions (see Fig. 2 G and H). Interestingly, the lactate accumulation rate of Day 3 feeding was found to be the lowest when compared against Day 2 feeding and Day 4 feeding. Altogether, the results obtained from employing different feeding volumes (Fig. 2 A) and different initial feeding days (Fig. 2 E) suggest that cells exhibit more rapid substrate utilization and metabolic activity rates when nutrients are supplemented at excess levels. The data further confirm that waste metabolites generated through upregulated pathways can inhibit cellular growth due to lactate production (Chen et al., 2001; Sha et al., 2020), reactive oxygen species generation (Sha et al., 2020; Ha and Lee, 2000), and endoplasmic reticulum stress (Zhong et al., 2012). On the other hand, the study showed that lower feeding volume (condition 4) or later feeding day (condition 8) both result in higher peak cell density but a shorter culture period due to a shortage of nutrients. For the growth profile and consumption profiles of all other conditions studied in this HCD process development, interested readers can refer to Figure S 1.

Table 1
Culture feeding strategy for high cell density process development. Feeding strategy was designed with reference to the inoculation seeding volume (30 mL).

Condition	Initial Feeding Day	Feeding Volume (% Seeding Volume)
1	2	Low – 5%
2	2	Medium – 10%
3	2	High – 15%
4	3	Low – 5%
5	3	Medium – 10%
6	3	High – 15%
7	4	Low – 5%
8	4	Medium – 10%
9	4	High – 15%

Ultimately, the feeding strategy obtained from condition 5 was selected for future study due to its highest attainable IVCD across all the conditions tested.

3.2. Inhibitory metabolites identification: global metabolomics study

Hydrophilic metabolites were explored in the global metabolomic study. A rigorous ranking system was used to screen metabolites generated in a fed-batch process for their inhibitory impact. First, a MS2 score was calculated and assigned to each global metabolome feature, from which only features with MS2 score greater than 0.5 or RSD less than 0.1 were further considered for targeted metabolomics study and biological verification impact analysis. Since a metabolite can have multiple retention times due to different liquid chromatography conditions, only one metabolite was selected for data-mapping to the human metabolome database. The remaining metabolite candidates were then selected for toxicity tests and targeted metabolomic verification to obtain high-confidence identification of waste inhibitory metabolites. For further detail regarding metabolomics information, interested reader can refer to Table S 3. The final list of all fifteen high-confidence metabolites is shown in Table 1. The global metabolomics analysis study was also repeated for CHO batch process.

3.3. Inhibitory metabolites identification: metabolites screening for impact

The first level of screening through spike-in study was performed in CHO-K1 batch cultures at two concentrations of metabolite (1 mM and 5 mM) in the initial growth medium. The rationale behind the selection of these initial concentrations was two-fold: i) high cell density CHO culture was observed to exhibit accumulation of metabolic by-products in the range of micromolar to a few millimolar amount in their extracellular environment based on previous study, and ii) previous study has verified certain metabolite candidate to show potential inhibitory effect on CHO growth 1 mM and 5 mM concentrations (Mulukutla et al., 2017).

The pH of the initial growth medium was initially measured (pH = 6.95), to which the pH of each experimental condition was adjusted to ensure no inhibitory effects due to pH shifts resulting from the respective metabolite addition. Cell culture growth parameters such as viable cell density (VCD) and viability (%) were monitored in which each of the cell cultures supplemented with the target metabolite at these two different concentrations were compared with the un-supplemented control cell cultures. A metabolite was therefore considered toxic to the cells if the VCD was lowered by more than or equal to 15% compared to the control in either the exponential or the stationary phase of cell culture.

For the metabolites impact screening study, ornithine and hypoxanthine were not included in the metabolite candidates spiking list due to their known physiological roles as substrates in cellular metabolism (Chen et al., 2012; Zajac et al., 2010). The remaining fifteen metabolites obtained from untargeted global metabolomics analysis were selected for biological verification to evaluate the toxicity effect on cellular performance in a standard culture bioprocess. The task was undertaken to provide a mean to mitigate the generation of metabolite that was observed to accumulate at high concentration during stationary phase of CHO fed-batch culture, of which their metabolic build-up does not contribute to cellular performance. Metabolites that show no inhibitory effect on CHO cultures, elucidated through spike-in study, would not be further considered in downstream metabolomics pipeline towards structural verification through targeted metabolomics and subsequent level determinations. The metabolites included in the spike-in study (and their abbreviations) are provided along with the rationale of identification confirmation or removal (see Table 2). The inhibitory impact on cellular performance due to spiking of metabolites presented as VCD impact heatmap is shown in Fig. 3 B. Of the fifteen metabolites considered for biological verification, hydroxyphenyllactic acid (HPL), deoxycytidine (DCI), l-allotheonine (LAT) were removed from the

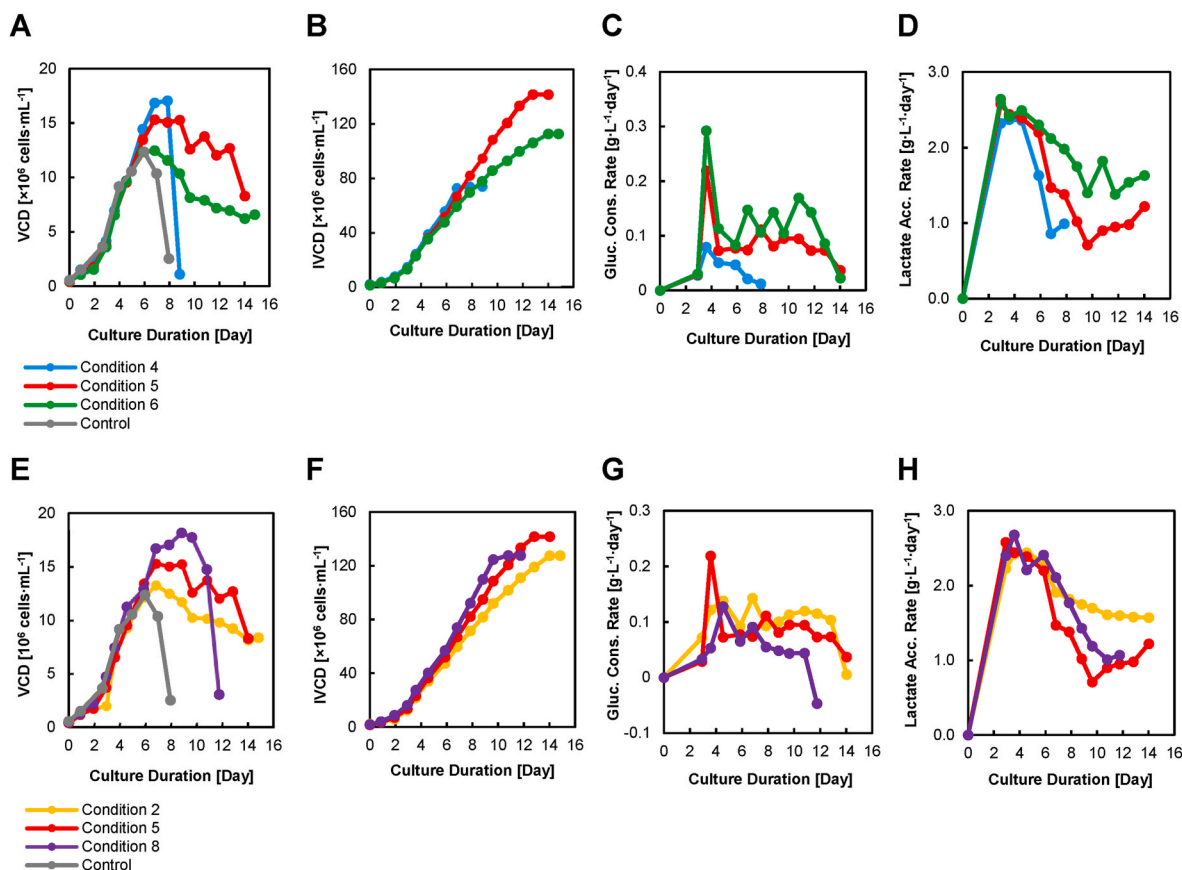


Fig. 2. High cell density fed-batch process development. (A) VCD, (B) IVCD, (C) Glucose consumption profile, and (D) Lactate accumulation profile of CHO-K1 cells cultivated in fed-batch process at different feeding volume. (E) VCD, (F) IVCD, (G) Glucose consumption profile, and (H) Lactate accumulation profile of CHO-K1 cells cultivated in fed-batch process at different initial feeding day. For HCD process development, a batch culture was also performed as a control to evaluate cellular performance and growth characteristics. Feeding volume was referenced to the initial 30 mL initial seeding volume. Fed-batch process was conducted at 5×10^5 cells·mL⁻¹ seeding density in 30 mL culture volume. For all conditions, the initial seeding day was assigned to be Day 0. Culture samples were collected before feeding each day, of which data sampling analysis was performed and reported. For study of the optimal feeding volume (A to D), three different feeding volume strategies were employed: condition 4 (1.5 mL feeding), condition 5 (3 mL feeding) and condition 6 (4.5 mL feeding). For study of the optimal feeding day, three different feeding day strategies were employed: condition 2 (Day 2), condition 5 (Day 3) and condition 8 (Day 4).

Table 2

LC-MS/MS data for inhibitory metabolite candidates accumulated in a fed-batch process from targeted metabolomics study. Candidates that could not be structurally verified in the end-of-culture samples were removed from the candidate list. The metabolic pathways the metabolites appear in is also listed. Mass fragments were ordered based on the intensity of the fragments signal in MS2 spectrum.

	Metabolite Name	RT [min]	m/z	MS1	MS2	MS3	Removed	Media [μ M]	End-of-culture [μ M]
Negative	Indole-3-carboxylic acid	1.7	160.0411	116.05			No	0	2.5
	Glutaric acid	2.45	131.0339	87.05	113.03	69.04 ^a	Yes, MS3	0	Not selected
	Methylsuccinic acid	2.45	131.0339	87.05	113.03	69.04	No	0	13.6
	Aconitic acid	3.96	173.0081	129.02	85.03	111.01	No	0	14.4×10^3
	trans-Cinnamic acid	1.79	147.0441	145.00	103.6	76.97 ^a	Yes, MS3/RT	0	Not selected
	2-Hydroxyisocaproic acid	1.75	131.0703	85.07	69.04		No	0	64.1
Positive	Trigonelline	10.31	138.0550	94.07	92.05	110.06	No	0	0.8
	p-Aminobenzoic acid	1.8	138.0550	65.04	77.04	94.07 ^a	Yes - MS3	0	Not selected
	N-Acetylputrescine	13.2	131.1179	114.09	72.08		No	0	0.2
	Cytidine monophosphate	15.87	324.0591	112.05	95.02	76.32	No	0	11.3
	Guanosine monophosphate	15.89	364.0653	152.06	135.03	110.04	No	0	20.0

^a Here, the intensity of the peak found from the MS3 spectra of the metabolite obtained from culture sample was significantly lower than that of the reference standard, which suggests the removal of the candidate metabolite from the feature list. For a further and more comprehensive review, interested readers can refer to Table S1.

metabolite candidates list since spiking of these metabolites into CHO cultures showed no inhibitory impact on cellular performance as shown in the VCD impact heatmap illustrated in Fig. 3 B. Additionally, 6-aminocaproic acid (6CA) was also removed due to having high RSD value (inconsistent MS data intensity) across replicate runs. Finally, glutaric acid (GA), trans-cinnamic acid (TCA), and p-aminobenzoic acid (pAA)

were removed from the metabolite candidates list through comparison of their MS3 spectrum and LC retention time obtained from the sample to the reference standard, after which the concentration at the end of culture was measured (see Table 2). For comparison of the MS3 spectrum between the candidate features, interested readers can refer to Table S 3.

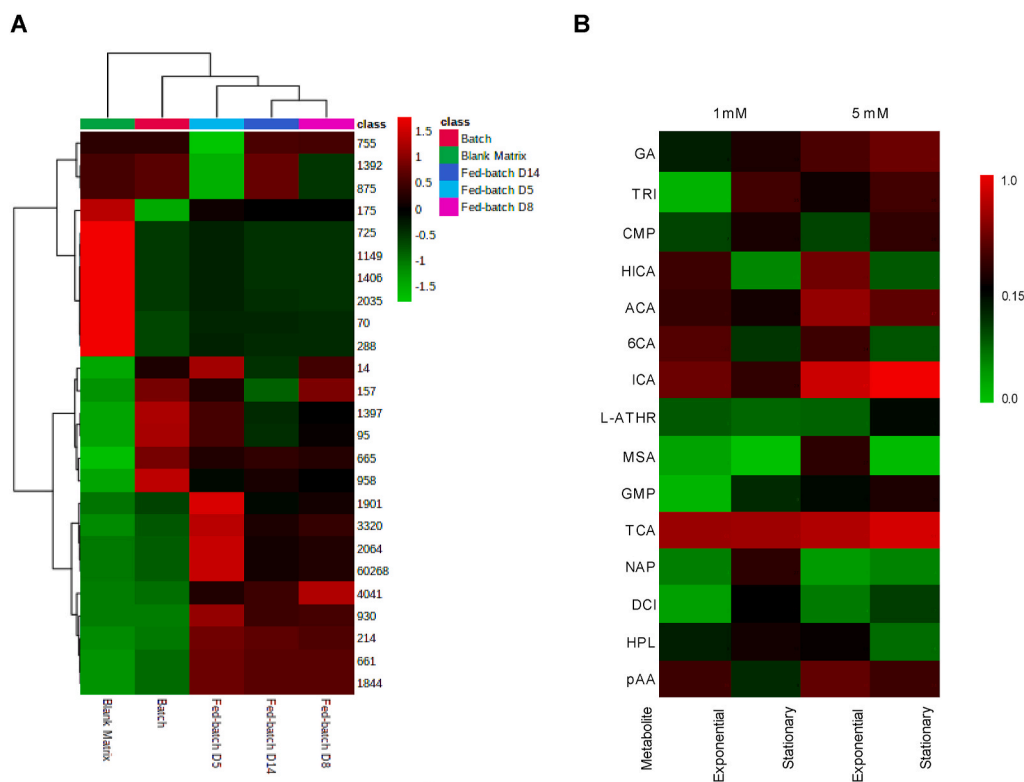


Fig. 3. [PRINT IN COLOR] Untargeted global metabolomics study of CHO-K1 cells. (A) Ion intensity heatmap of inhibitory metabolite candidates with high data quality. For each metabolite candidate, the ion intensity of metabolomics data was normalized against the median value and logarithmically transformed through MetaboAnalyst 5.0. Red (■) indicates higher relative ion intensity, and green (■) indicates smaller value of relative ion intensity, both scaled with mean-centered method. Class numbers represent metabolites ID based on human metabolome database (HMDB). (B) Overview of spike-in impact screening study. Matrix cells were colored based on their relative impact on cellular VCD. Red (■) indicates metabolite compounds that suppress cellular VCD by more than or equal to 15%, and green (■) indicates metabolite compounds that show no impact on cellular VCD, both compared against the control in exponential phase and/or stationary phase. (For interpretation of the references to color in this figure legend, the reader is referred to the Web version of this article.)

3.4. Inhibitory metabolites characterization in CHO-K1 and CHO-GS batch process

Verification on the identity of waste metabolites and quantification of their accumulated concentration in CHO batch culture was performed through targeted metabolomics study. Overall, careful study on the metabolism of cells allowed identification of eight metabolites accumulating at high level in the harvested samples. The impact of these metabolites on culture performance was further characterized in batch and fed-batch culture of CHO-K1, as well as batch culture of CHO-GS and HEK293 to determine whether the toxicity on cellular performance is universal across different mammalian cell lines. Overall, careful analysis of these metabolites of interest enabled a broader classification on the metabolic pathways responsible for their accumulation. The identities of the metabolites and their respective metabolic pathway are shown Fig. 4. The cellular level of metabolites accumulation as measured from samples obtained at the harvest day of CHO-K1 batch process is shown in Table 2.

The results obtained from the spiking studies of CHO-K1, and CHO-GS process are shown in Fig. 5 and Fig. 6. Here, metabolites CMP, GMP and ACA (aconitate) are known to accumulate from pathways emerging from the central carbon metabolism, such as the TCA cycle, purine, and pyrimidine metabolism. Of the three central carbon intermediates, the study showed that only CMP was shown to have a negative effect on cell growth at all tested concentrations while GMP and ACA were toxic at two concentration levels (1 mM and 5 mM) and one concentration level (1 mM) respectively out of the three concentrations that were tested. Surprisingly, the negative impact of ACA on cell growth was only found in cultures where ACA was supplemented in lower concentrations. At 5 mM spiking concentration to batch process, ACA showed a positive

impact on cell growth. It is also important to note that, cultures spiked with ACA showed a decrease in specific productivity along with CMP and GMP when tested at “cell” concentration (see Fig. 5 J). Overall, at the end-of-culture (“cell”) concentration noted in Table 2, the three metabolites CMP, GMP and ACA had an impact on CHO cell cultures, although the toxic effect due to GMP to cells was only significant at millimolar levels (see Fig. 5 A and Fig. 6 B). Thus, it was concluded from the study that CMP and GMP are growth inhibitors as well as productivity inhibitors. In the case of ACA (aconitate), this metabolite is generated as a TCA cycle intermediate which is formed during the conversion of citrate to iso-citrate catalyzed by mitochondrial aconitase (Aco2) in mammalian cells. Previous studies conducted on CHO process revealed that knockout of Aco2 negatively impacts cell growth (Dhami et al., 2018). This infers that supplementing ACA to cells drives the activity of TCA cycle in the forward direction to generate more ATP required for growth and protein production. Hence, ACA showed no growth toxicity and reduced productivity in CHO cells at “cell” concentration and in fact, at 5 mM enhanced growth in comparison to the control (see Fig. 5 C).

Of the eight identified toxic metabolites, HICA and MSA can be classified as emerging from the branched-chain amino acids (BCAA) which include isoleucine, leucine, and valine. HICA is the degradation product of leucine, and MSA is formed from the isomerization product of isoleucine. From our study, both compounds were observed to have a toxic effect on growth, with HICA showing a slightly higher toxicity as compared to MSA. Likewise, the negative effect on productivity of these two metabolites is less than five percent which makes them predominantly growth inhibiting metabolites (see Fig. 5 I and J). Historically, branched-chain amino acid metabolites (such as isovaleric acid) have been shown to be toxic to CHO cellular growth in fed-batch cultures (Li

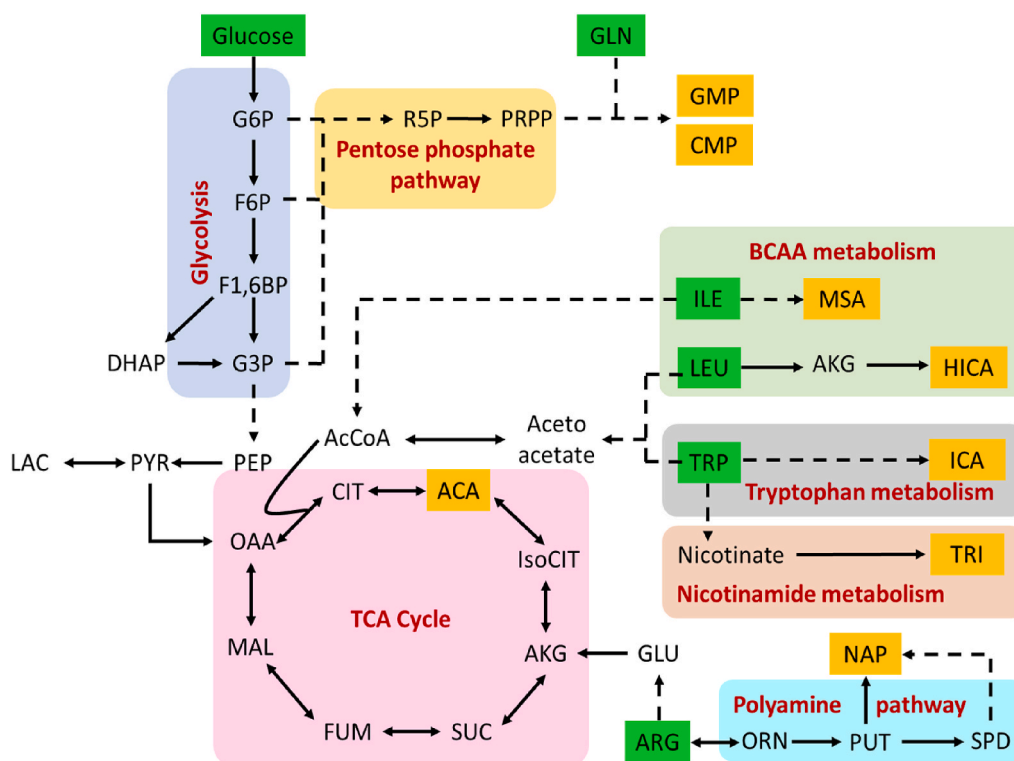


Fig. 4. [PRINT IN COLOR] Metabolites Generation Pathway and Metabolic Network Mapping in Mammalian Systems. Mapping of identified metabolites and their pathway of generation to CHO metabolic network. (For interpretation of the references to color in this figure legend, the reader is referred to the Web version of this article.)

et al., 2010). However, to the best of our knowledge, there was no literature evidence showing these novel metabolites secreted at toxic level to cell growth through BCAA degradation pathway during fed-batch culture, which highlights the current metabolomic study as an exhaustive effort to characterize CHO cellular metabolism in different culturing settings.

Other growth medium components supplemented to CHO cells (such as arginine, tryptophan, and vitamin B12) have also been linked to the identified toxic compounds (i.e., NAP, ICA and TRI). Of the three metabolites, ICA was previously reported to secret at high level into cell culture environment in CHO-GS cell line (Li et al., 2010). It was also shown in the same study that reduction of ICA through modulation of amino acid concentration or elimination of ICA production through cell line engineering could improve CHO cellular performance. Similar finding was observed in this current metabolomics study where ICA was found to be eminently toxic to cellular performance when supplemented at high level and moderately toxic at concentration up to 1 mM (see Fig. 5 B), although it has only been reported from literature that accumulation of ICA in the spent media was less than 10 μ M concentration. At 5 mM spiking concentration, ICA was reported to completely inhibit cellular growth. This tryptophan degradation metabolic product also decreased cellular productivity (see Fig. 5 J) when supplemented at micromolar level into CHO cultures corroborating the toxicity of ICA to these cell lines.

Finally, TRI and NAP which are generated as by-products of the nicotinate and arginine metabolism, respectively, were observed to be toxic to cells at lower concentration. Particularly in the study, NAP was shown to inhibit cellular growth at the measured cellular concentration (0.6 μ M). When supplemented back into cell culture at millimolar level, the toxic effect was not observed, which suggests that NAP was re-directed into the arginine metabolism pathway. Specifically, NAP potentially can be converted back to putrescine which is a substrate from the polyamine pathway (see Fig. 4 and Figure S2), which generates growth factors to promote cell proliferation in mammalian systems

(Hölttä and Pohjanpelto, 1982) and thereby neutralizing the inhibitory effect of NAP on cell growth, as shown in Fig. 5 B. Alternatively, excess NAP could also drive the metabolic flux in the forward direction downstream of its formation and be utilized by cells to support growth. In a similar fashion, TRI was found to be less toxic as the concentration increased from micromolar level to millimolar level. TRI is a metabolite by-product of nicotinate metabolism, which is a part of vitamin and cofactor metabolism. Since these chemical compounds are supplemented in lower amount in the growth media, trace amount (about a few μ M) of their metabolic by-products was shown to negatively impact cellular performance in the current study. Thus, with the aid of spiking in inhibitor spiked-in growth medium at varied concentration, the conducted study was able to characterize the varied impact of the identified metabolites on CHO cultures. The impact of the eight identified metabolites in higher cell density culture often found in fed-batch process was further examined in subsequent study as detail below.

3.5. Inhibitory metabolites characterization in CHO-K1 fed-batch process

In a standard industrial culture bioprocess, cells are exposed to inhibitory metabolites for an extended culture period as cells are cultivated in fed-batch mode. Thus, as an effort to validate metabolite inhibitory impact in a long-term process at higher cell density, a fourteen days fed-batch process with metabolites spiked in on Day 0 was performed. Cultivation strategy of cells followed closely to the method previously described in Section 2.1. Feeding strategy was designed based on the best performing condition as studied in the HCD fed-batch process development, namely feeding of 3 mL enriched medium B (10% of inoculation volume) starting on Day 3. Metabolites were spiked into fed-batch cultures on Day 0 at the end-of-culture concentration previously measured from samples obtained on Day 14 from the HCD fed-batch process, as shown Table 2. In this study, ICA which was proven as a growth inhibitor in past study was used as a positive inhibitor control (Mulukutla et al., 2017).

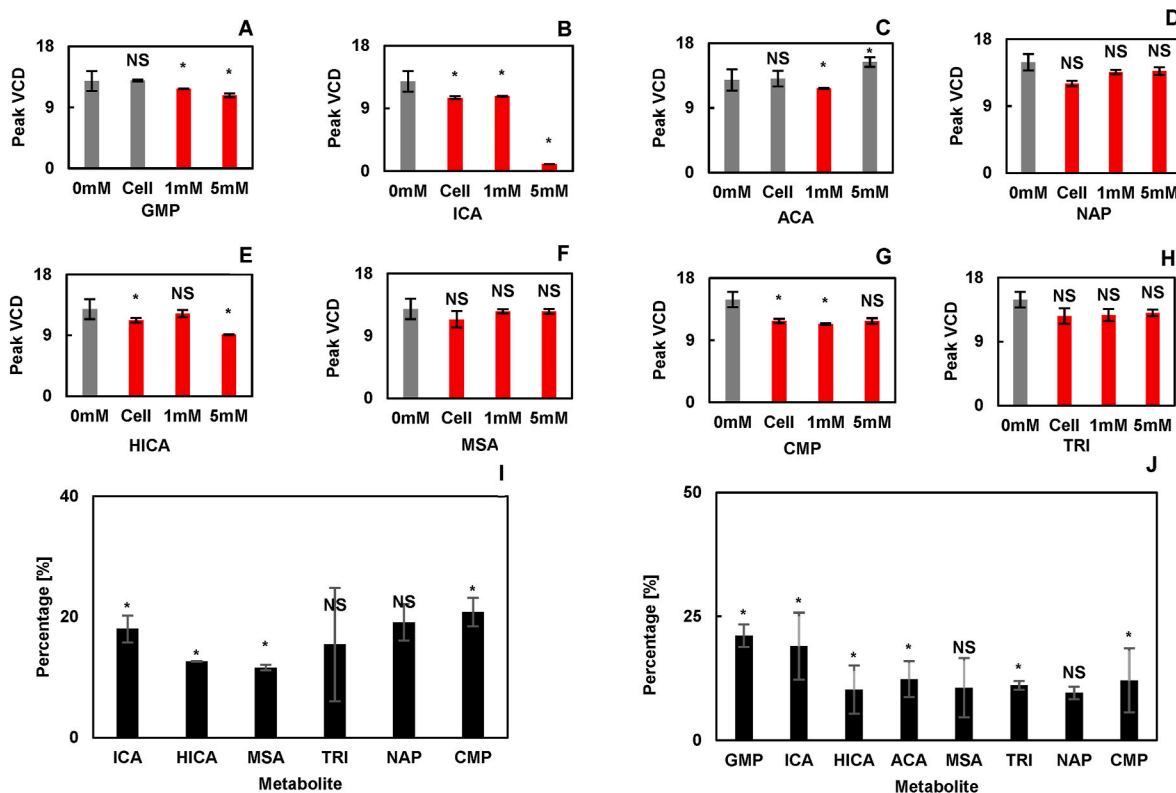


Fig. 5. Inhibitory impact on cellular performance at different spiking concentration in a CHO-K1 batch process. In this study, the impact on cellular performance due to spiking of (A) GMP, (B) ICA, (C) ACA, (D) NAP, (E) HICA, (F) MSA, (G) CMP, (H) TRI in CHO-K1 culture at different concentrations (cell – amount accumulated at end of culture level as measured, 1 mM and 5 mM). Red (■) indicates decrease in performance when compared to the control. (I) Percentage decrease in growth due to toxic metabolites when supplemented at “cell” concentration in batch cultures with respect to the control (*GMP and ACA had no effect on growth at “cell” levels*), and (J) Percentage decrease of antibody titer productivity (qP) due to spiking of metabolites at “cell” concentration levels in batch cultures with respect to the control. For cell level, metabolites were spiked at the following concentration: GMP (20 μ M), ICA (2.5 μ M), ACA (14.4 mM), NAP (0.2 μ M), HICA (64.1 μ M), MSA (13.6 μ M), CMP (11.3 μ M), and TRI (0.8 μ M). Bars mean \pm s.d.; n = 2, *p < 0.1. Statistics by two-tailed *t*-test against the control. (For interpretation of the references to color in this figure legend, the reader is referred to the Web version of this article.)

At the end of the growth phase (Day 4), the VCD across all culture conditions were experimentally measured (Fig. 7 A) and IVCD for each condition was calculated (Fig. 7 B). Overall, conditions spiked with inhibitory metabolites previously identified from the batch study showed a lower growth profile as compared against the control (without spiking of metabolites). Except for the ACA spiked condition, the remaining cultures showed more than 10% IVCD decrease when compared against the control (see Fig. 7 C). From the study, it was shown that of the seven metabolites, MSA, CMP and ICA appeared to pose a stronger inhibitory impact on cell density (IVCD decrease of 24.2%, 23.2%, and 22.0% in comparison to the control, respectively).

3.6. Productivity and product quality

Monoclonal antibody production was measured from samples collected at the harvest day from the fed-batch process. Overall, titer production for cultures spiked with HICA, CMP, TRI, ICA, NAP, and MSA showed more than 10% decrease in productivity when compared against the control (see Fig. 7 D to F). Product quality was also evaluated through measurement of the antibody glycosylation pattern. All cultures spiked with growth inhibitory metabolites showed more than 10% decrease in G1F formation and 50% decrease in G2F formation (see Fig. 7 G and H, for calculated percentage decrease, interested readers can refer to Table S4). The obtained data altogether suggest that the identified metabolites inhibit the attachment of fucose to n-acetylglucosamine. Additionally, the analysis also reveals the absence of G2F glycosylation in cultures spiked with HICA.

3.7. Validation of inhibitory metabolites in multiple mammalian cell lines

Accumulation of inhibitory metabolites during growth and production phase was also studied in different mammalian cell lines capable of expressing therapeutic proteins. Here, six of the eight novel inhibitory metabolites that accumulated during CHO-K1 fed-batch process were also found to accumulate in CHO-GS and HEK293 bioprocess. The accumulation concentration measured at harvest day was shown in Table 3. The results suggest that metabolites identified using untargeted and targeted metabolomics strategy as shown here are not strictly exclusive to CHO-K1 but can also be found across multiple mammalian systems used to express therapeutic proteins.

Interestingly, the concentration of the inhibitory metabolite ACA that accumulated during the cultivation of CHO-GS and HEK293 system is lower compared to CHO-K1. An examination of the metabolism of the individual cell lines may help to explain the observed accumulation trend of different metabolites across these cell lines. For CHO-GS, glutamine synthetase expressed during transcription allows glutamine being resynthesized from glutamate which likely lowers the deamination activity of converting glutamate into α -ketoglutarate, therefore decreasing the amount of α -ketoglutarate available for the TCA cycle. Reduction of α -ketoglutarate may require upregulation of other upstream enzymatic activity to provide adequate protons for the TCA cycle. In other mammalian system, this could be achieved through higher metabolic activity of proline which yields α -ketoglutarate as the direct beneficial by-product. However, as CHO is known to be dysfunctional in metabolism of proline, other enzymatic activity pathways must be upregulated to account for the reduction in

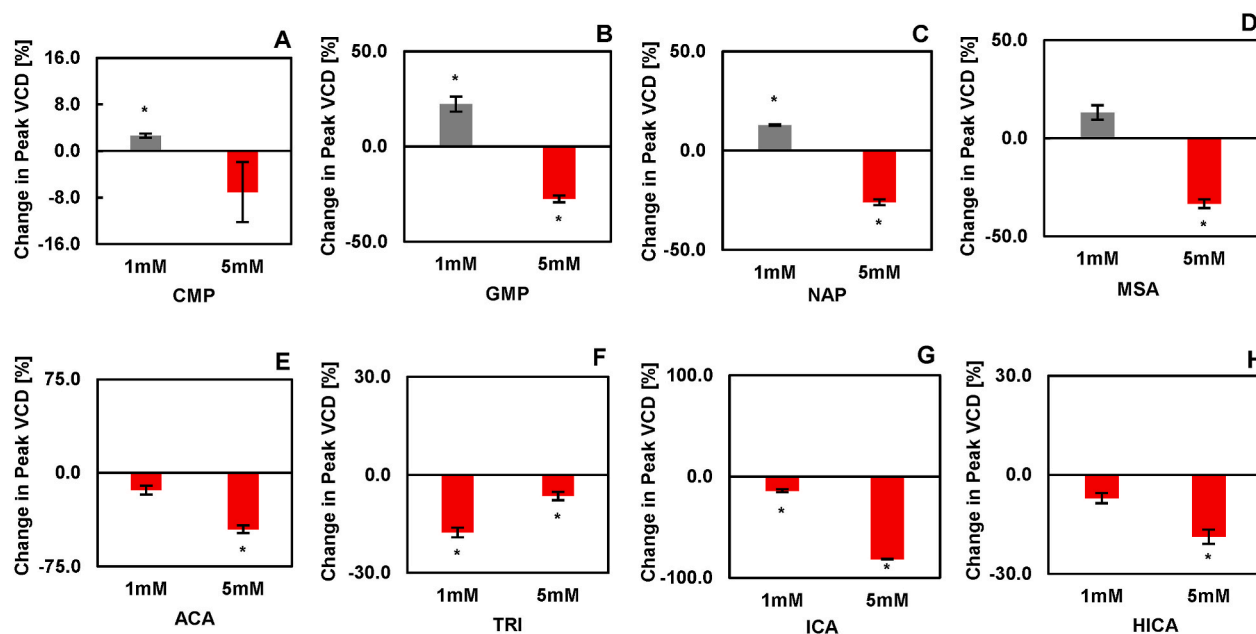


Fig. 6. Inhibitory Impact on Cellular Performance at Different Spiking Concentration in a CHO-GS Batch Process. As shown here, the impact on cellular performance due to spiking of (A) CMP, (B) GMP, (C) NAP, (D) MSA, (E) ACA, (F) TRI, (G) ICA, and (H) HICA into CHO-GS culture at different concentrations (1 mM and 5 mM) was studied. Here, for metabolites (A) to (D), negative impact on growth was only observed at 5 mM spiking concentration, whereas for metabolites (E) to (H), cellular growth was negatively impacted at both 1 mM and 5 mM spiking concentrations. Red (■) indicates decrease in performance when compared to the control. Bars mean \pm s.d.; $n = 2$, * $p < 0.1$. Statistics by two-tailed t -test against the control. (For interpretation of the references to color in this figure legend, the reader is referred to the Web version of this article.)

α -ketoglutarate, one of which is aconitase activity (Valle et al., 1973). Aconitase is known to facilitate the consumption of aconitate to form isocitrate which is precursor to formation of α -ketoglutarate. Thus, upregulation of aconitase activity reduces the accumulation of aconitate, and hence explains of the reduction in culture concentrations of the metabolite ACA observed in the case of CHO-GS.

Regarding the decrease in the accumulation of ACA in the case of HEK293, a further look into the metabolic system of HEK293, suggests a plausible explanation for the observed trend. For HEK293, the expression of the *c-MYC* regulator gene could account for increasing the intracellular concentration of pyrroline-5-carboxylate reductase (PYCR) (Tanner et al., 2018). As PYCR facilitates the breaking down of 1-pyrroline-5-carboxylate (P5C) in the proline cycle, additional availability of PYCR may drive the accumulation of P5C followed by a consequential reduction in glutamate (Le Chatelier's principle), and ultimately, leading to a decrease in the amount of α -ketoglutarate. The rest of the pathway follows similar reasoning as made above for CHO-GS which ultimately accounts for the observed reduction of ACA available in the TCA cycle. Interestingly, while ACA was found to accumulate in both HEK293 and CHO-GS throughout the culture duration, the measured concentration of ACA at harvest day was found to be lower in HEK293 compared to CHO-K1. Difference in level of gene expression and enzymatic activity between CHO-K1 and HEK system may provide an explanation for the differences in levels between these two hosts. As mentioned above, CHO metabolic systems are known to be proline auxotrophic which prevent any production of α -ketoglutarate through this pathway. This, however, is not the case for HEK293, therefore excess amount of α -ketoglutarate yielded from the proline metabolism cycle found in HEK293 would drive the equilibrium of the consumption reaction of ACA to the right (Le Chatelier's principle), therefore reducing the accumulation of ACA at throughout the culture duration. A more in-depth analysis is needed to be conducted in future study to verify the observed trend in metabolites accumulation in HEK293 cell line.

The concentration of CMP, TRI, and HICA were found to be more

abundant in CHO-GS. Depletion in the synthesis of α -ketoglutarate in CHO-GS due to CHO being proline auxotroph promotes the activity other relevant metabolic pathways, namely glycolysis and the metabolism of other amino acids, including leucine and tryptophan. This would account for the increase in accumulated concentration at end-of-culture observed in the case of CMP (direct by-product of glycolysis), HICA (direct by-product from the metabolism of leucine), and TRI (direct by-product from the metabolism of tryptophan) observed throughout the study. These pathways are therefore activated to stimulate the production of α -ketoglutarate in the CHO-GS cell lines that are lost from activation of the glutamine synthase gene.

In order to evaluate if the inhibitors identified in the current study also exhibited an effect on cell growth for cell lines beyond CHO-K1, negative impact study on culture performance of CHO-GS process was conducted on the six metabolites already seen to accumulate in CHO-GS cultures (see Table 3) along with ICA and GMP. Similar to the previously conducted batch screening studies on CHO-K1 cell line, the metabolites were spiked in the CHO-GS cultures at two different concentrations (1 mM and 5 mM). Here, CHO-GS cells were cultivated in the second generation of medium A, hereby addressed as medium A 1.1 (medium A 1.1 includes similar amino acids as medium A 1.0 but eliminates or reduces other non-essential inputs). The results of the impact study of the metabolites on CHO-GS cell line study are shown in Fig. 6. The VCD profile of the condition with inhibitory metabolites spiked in on Day 0 was compared against the control group. It was observed that all experimental conditions spiked with metabolites showed inhibition on cellular growth at higher concentration (5 mM) during both exponential and stationary phase of the culture process. A similar trend was also observed for most of the metabolites at lower (1 mM) concentration, except for GMP, NAP and TRI which only showed inhibition in cell growth during the early exponential phase at 1 mM concentration. The study demonstrates the universal nature of the identified metabolites as they were shown to generate during cellular metabolism and have an impact on growth across multiple mammalian cell lines when cultivated in different growth media.

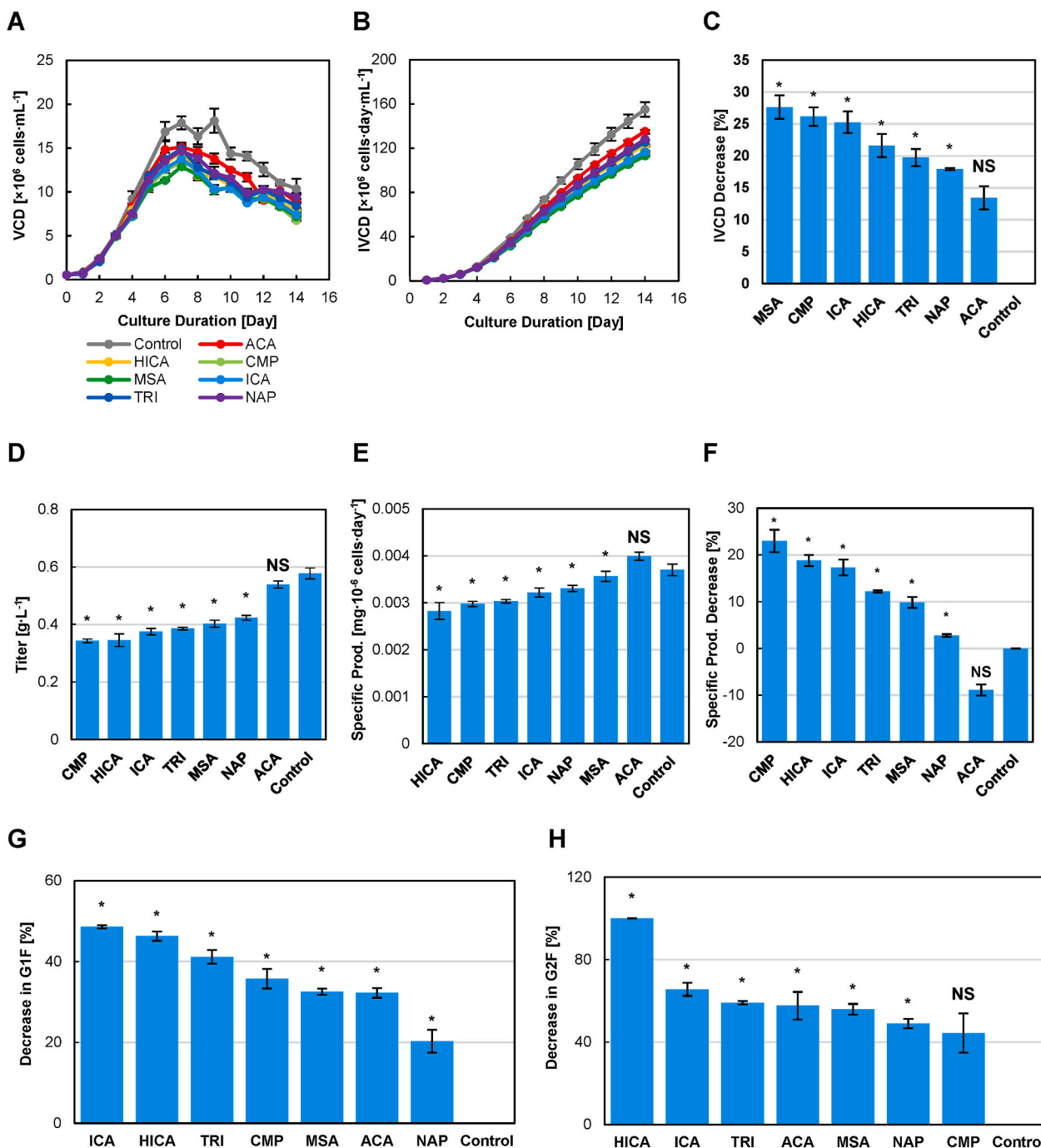


Fig. 7. Inhibitory impact on cellular growth and protein synthesis in CHO-K1 fed-batch process due to accumulation of metabolites. (A) VCD, (B) IVCD and (C) Percentage decrease in IVCD of cultures with inhibitory metabolites spiked in on the first day when compared against the control. (D) Titer production, (E) Specific productivity, (F) Percentage decrease in specific productivity of cultures with inhibitory metabolites spiked in on the first day when compared against the control, (G) Percentage decrease in G1F formation and (H) Percentage decrease in G2F formation. In this study, the inhibitory impact due to prolonged duration of exposure to metabolites in standard CHO fed-batch process was evaluated. Spiking concentration of metabolites as shown here: ACA (14.4 mM), HICA (64.1 μM), CMP (11.3 μM), MSA (13.6 μM), ICA (2.5 μM), TRI (0.8 μM), NAP (0.2 μM). Metabolites were spiked into CHO cultures on Day 0, of which the spiking concentration was previously determined from the measured end-of-culture accumulation level in a standard fed-batch bioprocess. Bars, mean \pm s.e.m.; $n = 3$, * $p < 0.05$; NS non-significant. Statistics by two-tailed t -test against the control.

Overall, this inhibitory impact study showed that accumulated inhibitors were found predominantly in fed-batch process, which suggests that reducing certain nutrient inputs might help to mitigate the accumulation of wasted inhibitory metabolites. Perhaps, the most crucial initial step is to identify and regulate inefficient metabolic fluxes occurring throughout glycolysis and amino acids consumption. Generation of inhibitory metabolites can then be best controlled during the

stage when they are generated and accumulated into the cytoplasm, prior to their release into the surrounding growth medium. Overall, the study indicates that accumulation of growth inhibitors secreted in a culture process can be controlled via up- or down-regulation of upstream metabolic fluxes where the end-of-culture metabolites was either consumed or generated. Further study regarding genetic intervention of the corresponding genes responsible for these metabolic pathways can

Table 3

Metabolite accumulation in CHO-K1, CHO-GS, and HEK293 production host at harvest day cultivated in batch process measured through LC-MS. Here, the reported molar concentration of each metabolite was normalized against the measured viable cell density.

	Concentration [$\mu\text{mole} \cdot 10^{-6}$ cells]					
	ACA	HICA	MSA	CMP	TRI	NAP
CHO-K1	24.6074	0.0750	0.0280	0.0826	0.0006	0.0011
CHO-GS	13.4884	0.7713	0.0632	1.9144	0.0198	0.0049
HEK293	17.4934	1.3447	0.0387	0.0607	0.0005	0.0042

perhaps offer a robust set of tools to control and manipulate the generation of growth inhibitory metabolites in a culture process of mammalian cells.

4. Conclusions

In conclusion, eight metabolites derived as by-products from the metabolism of nutrients in mammalian cells were verified to show inhibitory impact on CHO cells cultivated in batch and fed-batch process. Experimental study was conducted to verify of six of the identified eight metabolites to be novel growth inhibitors: aconitic acid (ACA), 2-hydroxyisocaproic acid (HICA), methylsuccinic acid (MSA), cytidine monophosphate (CMP), trigonelline (TRI), and n-acetyl putrescine (NAP). Metabolites spiking study on CHO batch process was conducted at 1 mM and 5 mM spiking concentration. At both tested concentrations, seven out of eight metabolites (ACA, CMP, GMP, HICA, ICA, MSA and NAP) were toxic to cellular growth, whereas four out of eight (NAP, TRI, CMP and GMP) showed negative impact on titer productivity. Spiking study was also conducted on CHO fed-batch cultures at cellular accumulated level in a fed-batch process. Except for ACA, all metabolites were shown to have inhibitory impact on the growth profile, with three metabolites (MSA, CMP and ICA) showing significant degree of growth suppression. Regarding protein production, six metabolites (HICA, CMP, TRI, ICA, NAP, MSA) showed inhibitory impact on specific titer productivity and IgG glycosylation profile. Consequentially, suppression in glycosylated activity also suppressed the galactosylation profile, which were shown in the study to inhibit the formation of mono-galactosylated biantennary (G1F) and biantennary galactosylated (G2F) N-glycans, with a more profound impact on the latter as expected due to the additional requirement of a galactose subunit. Spiking study was also repeated on CHO-GS cell line. Of the eight metabolites included in the study, only four (CMP, GMP, NAP and MSA) showed negative impact on cellular growth at 5 mM spiking concentration. The remaining metabolites (ACA, TRI, ICA, HICA) showed growth suppression at both 1 mM and 5 mM spiking concentrations. Overall, the study suggests that accumulation of growth inhibitors secreted in cell culture process can be controlled via up- or down-regulation of upstream metabolic fluxes where the metabolites accumulated at the end-of-culture was either consumed or generated. Future studies, such as genetic intervention of the corresponding genes responsible for these metabolic pathways can perhaps offer a robust set of tools to control and manipulate the generation of growth inhibitory metabolites in a culture process of mammalian cells.

Author statement

Bingyu Kuang: Conceptualization, Methodology, Investigation, Formal analysis, Validation, Writing- Original Draft, Writing – Review & Editing, Visualization; **Venkata Gayatri Dhara:** Conceptualization, Methodology, Investigation, Formal analysis, Validation, Writing- Original Draft, Writing – Review & Editing, Visualization; **Duc Hoang:** Investigation, Formal analysis, Validation, Writing- Original Draft, Writing – Review & Editing; **Jackson Jenkins:** Investigation, Formal analysis, Validation, Writing- Original Draft, Writing – Review &

Editing; **Pranay Ladiwala:** Investigation, Formal analysis, Validation, Writing- Original Draft, Writing – Review & Editing; **Yanglan Tan:** Methodology, **Scott Shaffer:** Methodology, **Shaun Galbraith:** Conceptualization, Methodology, Investigation, Writing- Original Draft; **Michael Betenbaugh:** Conceptualization, Methodology, Investigation, Writing- Original Draft, Writing – Review & Editing, Supervision, Project administration, Funding acquisition; **Seongkyu Yoon:** Conceptualization, Methodology, Investigation, Writing- Original Draft, Writing – Review & Editing, Supervision, Project administration, Funding acquisition;

Declaration of competing interest

The authors declare that they have no known competing financial interests or personal relationships that could have appeared to influence the work reported in this paper.

The authors declare the following financial interests/personal relationships which may be considered as potential competing interests:

Acknowledgements

This work was funded and supported by Advanced Mammalian Biomanufacturing Innovation Center (AMBIC) through the Industry – University Cooperative Research Center Program under U.S. National Science Foundation (Grant number: 1624684). We would like to express our gratitude to all AMBIC member companies for their mentorship and financial support.

Appendix A. Supplementary data

Supplementary data related to this article can be found at <https://doi.org/10.1016/j.mec.2021.e00182>.

Conflict of interests

All the authors declare no conflict of interest.

Declaration of interest

None.

References

- Arden, N., Betenbaugh, M.J., 2004. Life and death in mammalian cell culture: strategies for apoptosis inhibition. *Trends Biotechnol.* 22 (4), 174–180. <https://doi.org/10.1016/j.tibtech.2004.02.004>.
- Buchsteiner, M., et al., 2018. Improving culture performance and antibody production in CHO cell culture processes by reducing the Warburg effect. *Biotechnol. Bioeng.* 115 (9), 2315–2327. <https://doi.org/10.1002/bit.26724>.
- Chen, P., Harcum, S.W., 2005. Effects of amino acid additions on ammonium stressed CHO cells. *J. Biotechnol.* 117 (3), 277–286. <https://doi.org/10.1016/j.jbiotec.2005.02.003>.
- Chen, K., et al., 2001. Engineering of a mammalian cell line for reduction of lactate formation and high monoclonal antibody production. *Biotechnol. Bioeng.* 72 (1), 55–61. [https://doi.org/10.1002/1097-0290\(20010105\)72:1<55::aid-bit8>3.0.co;2-4](https://doi.org/10.1002/1097-0290(20010105)72:1<55::aid-bit8>3.0.co;2-4).
- Chen, F., et al., 2012. Insight into the roles of hypoxanthine and thymidine [corrected] on cultivating antibody-producing CHO cells: cell growth, antibody production and long-term stability. *Appl. Microbiol. Biotechnol.* 93 (1), 169–178. <https://doi.org/10.1007/s00253-011-3484-z>.
- Chong, W.P., et al., 2011. Metabolomics-based identification of apoptosis-inducing metabolites in recombinant fed-batch CHO culture media. *J. Biotechnol.* 151 (2), 218–224. <https://doi.org/10.1016/j.jbiotec.2010.12.010>.
- Chong, W.P., et al., 2012. LC-MS-based metabolic characterization of high monoclonal antibody-producing Chinese hamster ovary cells. *Biotechnol. Bioeng.* 109 (12), 3103–3111. <https://doi.org/10.1002/bit.24580>.
- Dhami, N., et al., 2018. Mitochondrial aconitase is a key regulator of energy production for growth and protein expression in Chinese hamster ovary cells. *Metabolomics* 14 (10), 136. <https://doi.org/10.1007/s1306-018-1430-0>.
- Dhara, V.G., et al., 2018. Recombinant antibody production in CHO and NS0 cells: differences and similarities. *BioDrugs* 32 (6), 571–584. <https://doi.org/10.1007/s40259-018-0319-9>.

- Freund, N.W., Croughan, M.S., 2018. A simple Method to Reduce both lactic Acid and ammonium Production in industrial animal cell culture. *Int J mol sci*, 19 (2), 385. <https://doi.org/10.3390/ijms19020385>.
- Grilo, A.L., Mantalaris, A., 2019. The increasingly human and profitable monoclonal antibody market. *Trends Biotechnol.* 37 (1), 9–16. <https://doi.org/10.1016/j.tibtech.2018.05.014>.
- Ha, H., Lee, H.B., 2000. Reactive oxygen species as glucose signaling molecules in mesangial cells cultured under high glucose. *Kidney Int. Suppl.* 77, S19–S25. <https://doi.org/10.1046/j.1523-1755.2000.07704.x>.
- Hiller, G.W., et al., 2017. Cell-controlled hybrid perfusion fed-batch CHO cell process provides significant productivity improvement over conventional fed-batch cultures. *Biotechnol. Bioeng.* 114 (7), 1438–1447. <https://doi.org/10.1002/bit.26259>.
- Hoang, D., et al., 2021. Characterization of Chinese hamster ovary cell culture feed media precipitate. *Biotechnol. Prog.* e3188. <https://doi.org/10.1002/btpr.3188> n/a (n/a): p.
- Hölttä, E., Pohjanpelto, P., 1982. Polyamine dependence of Chinese hamster ovary cells in serum-free culture is due to deficient arginase activity. *Biochimica et Biophysica Acta (BBA) - molecular Cell Research*, 721 (4), 321–327. [https://doi.org/10.1016/0167-4889\(82\)90085-4](https://doi.org/10.1016/0167-4889(82)90085-4).
- Huang, H., et al., 2020. IsoSearch: an untargeted and unbiased metabolite and lipid isotopomer tracing strategy from HR-LC-MS/MS datasets. *Methods Protoc* 3 (3), 54. <https://doi.org/10.3390/mps3030054>.
- Karst, D.J., et al., 2017. Intracellular CHO cell metabolite profiling reveals steady-state dependent metabolic Fingerprints in perfusion culture. *Biotechnol prog.*, 33 (4), 879–890. <https://doi.org/10.1002/btpr.2421>.
- Kunert, R., Reinhart, D., 2016. Advances in recombinant antibody manufacturing. *Appl. Microbiol. Biotechnol.* 100 (8), 3451–3461. <https://doi.org/10.1007/s00253-016-7388-9>.
- Lao, M.S., Toth, D., 1997. Effects of ammonium and lactate on growth and metabolism of a recombinant Chinese hamster ovary cell culture. *Biotechnol. Prog.* 13 (5), 688–691. <https://doi.org/10.1021/bp9602360>.
- Li, F., et al., 2010. Cell culture processes for monoclonal antibody production. *mAbs* 2 (5), 466–479. <https://doi.org/10.4161/mabs.2.5.12720>.
- Mohan, C., et al., 2008. Assessment of cell engineering strategies for improved therapeutic protein production in CHO cells. *Biotechnol. J.* 3 (5), 624–630. <https://doi.org/10.1002/biot.200700249>.
- Mohmad-Saberi, S.E., et al., 2013. Metabolomics profiling of extracellular metabolites in CHO-K1 cells cultured in different types of growth media. *Cytotechnology* 65 (4), 577–586. <https://doi.org/10.1007/s10616-012-9508-4>.
- Mulukutla, B.C., et al., 2017. Identification and control of novel growth inhibitors in fed-batch cultures of Chinese hamster ovary cells. *Biotechnol. Bioeng.* 114 (8), 1779–1790. <https://doi.org/10.1002/bit.26313>.
- Pereira, S., Kildegaard, H.F., Andersen, M.R., 2018. Impact of CHO Metabolism on cell Growth and protein production: an Overview of Toxic and inhibiting Metabolites and nutrients. *Biotechnol. J.* 13 (3), e1700499. <https://doi.org/10.1002/biot.201700499>.
- Polanco, A., Kuang, B., Yoon, S., 2020. Bioprocess Technologies that preserve the quality of iPSCs. *Trends Biotechnol.* <https://doi.org/10.1016/j.tibtech.2020.03.006>.
- Sha, S., et al., 2020. At-line N-linked glycan profiling for monoclonal antibodies with advanced sample preparation and high-performance liquid chromatography. *Journal of bioscience and bioengineering*, 130 (3), 327–333.
- Sha, S., Kuang, B., Yoon, S., 2020. Characterization of dynamic regulation in Chinese hamster ovary (CHO) cell cultures in the late exponential phase. *Biochemical engineering journal*, p. 107897. <https://doi.org/10.1016/j.bej.2020.107897>.
- Sun, X.M., Zhang, Y.X., 2001. [Effects of ammonia on cell metabolism in the culture of recombinant CHO cells]. *Sheng Wu Gong Cheng Xue Bao*, 17 (3), 304–309. <https://doi.org/10.1021/bp9602360>.
- Takagi, Y., et al., 2017. The enhancement of antibody concentration and achievement of high cell density CHO cell cultivation by adding nucleoside. *Cytotechnology* 69 (3), 511–521. <https://doi.org/10.1007/s10616-017-0066-7>.
- Tanner, J.J., Fendt, S.M., Becker, D.F., 2018. The proline cycle as a potential cancer therapy target. *Biochemistry* 57 (25), 3433–3444. <https://doi.org/10.1021/acs.biochem.8b00215>.
- Valle, D., et al., 1973. Proline biosynthesis: multiple defects in Chinese hamster ovary cells. *Biochem. Biophys. Res. Commun.* 53 (4), 1130–1136. [https://doi.org/10.1016/0006-291x\(73\)90582-2](https://doi.org/10.1016/0006-291x(73)90582-2).
- Zajac, A., et al., 2010. Arginine and ornithine supplementation increases growth hormone and insulin-like growth factor-1 serum levels after heavy-resistance exercise in strength-trained athletes. *J. Strength Condit Res.* 24 (4), 1082–1090. <https://doi.org/10.1519/JSC.0b013e3181d321ff>.
- Zhong, Y., et al., 2012. Activation of endoplasmic reticulum stress by hyperglycemia is essential for Muller cell-derived inflammatory cytokine production in diabetes. *Diabetes* 61 (2), 492–504. <https://doi.org/10.2337/db11-0315>.